The Three-Dimensional Structure and Evolution of a Tornado Boundary Layer

KAREN A. KOSIBA AND JOSHUA WURMAN

Center for Severe Weather Research, Boulder, Colorado

(Manuscript received 24 June 2013, in final form 15 August 2013)

ABSTRACT

The finescale three-dimensional structure and evolution of the near-surface boundary layer of a tornado (TBL) is mapped for the first time. The multibeam Rapid-Scan Doppler on Wheels (RSDOW) collected data at several vertical levels, as low as 4, 6, 10, 12, 14, and 17 m above ground level (AGL), contemporaneously at 7-s intervals for several minutes in a tornado near Russell, Kansas, on 25 May 2012. Additionally, a mobile mesonet anemometer measured winds at 3.5 m AGL in the core flow region. The radar, anemometer, and ground-based velocity-track display (GBVTD) analyses reveal the peak wind intensity is very near the surface at ~5 m AGL, about 15% higher than at 10 m AGL and 25% higher than at ~40 m AGL. GBVTD analyses resolve a downdraft within the radius of maximum winds (RMW), which decreased in magnitude when varying estimates for debris centrifuging are included. Much of the inflow (from -1 to -7 m s^{-1}) is at or below 10–14 m AGL, much shallower than reported previously. Surface outflow precedes tornado dissipation. Comparisons between large-eddy simulation (LES) predictions of the corner flow swirl ratio S_c and observed tornado intensity changes are consistent.

1. Introduction

The corner and boundary layer regions of tornadoes (e.g., Lewellen 1976, 1993; Snow 1982; Kessler 1986, 197–236; Davies-Jones et al. 2001) are the most difficult and most critical to sample because they are in direct contact with the underlying surface, cause damage, and dictate the vortex structure at low levels and perhaps through a significant depth of the tornado. Although mobile radar observations of the tornado core flow have become more frequent (e.g., Wurman et al. 1996; Wurman and Gill 2000, hereafter WG00; Bluestein et al. 2003; Bluestein et al. 2004; Lee and Wurman 2005, hereafter LW05; Wurman et al. 2007a, hereafter W07; Tanamachi et al. 2007; Kosiba et al. 2008, hereafter K08; Kosiba and Wurman 2010, hereafter KW10; Wakimoto et al. 2012, hereafter W12; Wurman et al. 2013a, hereafter W13; Wurman and Kosiba 2013), they commonly are >40 m AGL and inadequately sample the near-surface tornado boundary layer (TBL) (i.e., the lower portion of the boundary layer that may be impacted directly by frictional effects).

To observe the TBL with radar, it is necessary for that radar to be close to the tornado to mitigate the effects of beam spreading and intervening obstructions (e.g., terrain, structures, and foliage). On only rare occasions (e.g., W07) are observations obtained <10 m AGL. Ideally, near-surface three-dimensional radar observations in combination with surface in situ one-dimensional transects of the TBL would combine to provide a time-varying three-dimensional mapping. However, in situ wind observations are exceedingly difficult and hazardous to obtain due to the violence, unpredictable paths, and typically short lifespans of tornadoes (Wurman et al. 2013b, manuscript submitted to *Bull. Amer. Meteor. Soc.*). In the rare instances that both in situ and low-level radar wind observations have been obtained (e.g., W13), ground-relative wind speeds near the surface, V_g, are comparable to or even stronger than radar-measured winds, V_d, ~30 m AGL.

Numerical simulations (e.g., Lewellen et al. 1997; Lewellen et al. 2000, hereafter L00; Lewellen and Lewellen 2007, hereafter LL07) and laboratory models (e.g., Church et al. 1979) of tornadoes have been instrumental in understanding the TBL, but these results remain largely unverified observationally. Hoecker's (1960) video analysis of the flow in a tornado attempted to quantify the near-surface structure of a tornado. Using debris and cloud tags as tracers, radial inflow, $V_r < 0$, was identified below 152 m AGL, and maximized at 53 m

Corresponding author address: Dr. Karen A. Kosiba, Center for Severe Weather Research, 1945 Vassar Circle, Boulder, CO 80305. E-mail: kakosiba@cswr.org

DOI: 10.1175/WAF-D-13-00070.1

© 2013 American Meteorological Society

Unauthenticated | Downloaded 02/13/24 12:47 AM UTC

AGL. Doppler on Wheels (DOW; Wurman et al. 1997; Wurman 2001, 2008) radar data in one tornado did not reveal inflow ~30 m AGL (WG00), but it was suggested that centrifuging of debris (Dowell et al. 2005) may have masked the convergence signature. DOW data, taken at ~10 and 14 m AGL from two different tornadoes (W07; Alexander and Wurman 2005, hereafter AW05), revealed convergences of 0.10 and 0.06 s^{-1}, respectively, suggesting strong convergence (not fully masked by centrifuging) near the surface.

LW05, KW10, W12, and W13 have used the ground-based velocity-track display (GBVTD) (Lee et al. 1999) scheme to resolve three-dimensional tornado structure. LW05 revealed inflow from $z = 0$ to 1.15 km AGL in a large and violent tornado. W12 applied the GBVTD technique to DOW data from the second Verification of the Origins of Rotation in Tornadoes Experiment (VORTEX2; Wurman et al. 2012) in a tornado at two consecutive times. Initially, there was strong outflow, while 2 min later there was very weak inflow surrounding the tornado. An approximation for centrifuging of hydrometeors weakened the initial outflow and strengthened the later inflow. The large-eddy simulation (LES) of Lewellen et al. (2008) demonstrated that small debris could alter the wind speeds and tornado structure near the surface. Using GBVTD and numerical simulations, Nolan (2013) emphasized the need to represent accurately the low-level inflow and to account for debris centrifuging. The debris centrifuging velocity, V_{cf}, which depends on debris type, amount, density, shape, recycling, electrical/scattering characteristics, etc., currently is unknown, and can only be approximately accounted for in radar-based analyses.

W13 combined in situ anemometer wind measurements (in the same tornado analyzed by W12) at 3.5 m AGL with Rapid-Scan DOW (RSDOW; Wurman and Randall 2001) observations ≥30 m AGL to reconstruct the low-level tornado vortex structure. At 3.5 m AGL, strong radial inflow ($V_r \sim -40$ m s^{-1}) was present just outside the radius of maximum V_t (RMW), but at ~30 m AGL, radar analyses revealed little to no inflow. Integrated analyses revealed a divided vortex structure with an axial updraft near the surface and a downdraft aloft. No data were available between 3.5 and 30 m AGL, so the details of the vertical profile of the winds in these lowest, critical levels of the TBL are unknown. Peak anemometer-measured winds, $V_g = 58$ m s^{-1}, were more intense than those measured by radar ~30 m AGL. DOW observations from other tornadoes also suggested that the most intense velocities may occur <30 m AGL (W07). Except for W13, these previous radar-based analyses used conventionally scanned radar data, resulting in limitations due to possible errors resulting from rapid tornado evolution during the several 10s of seconds between observations at the lowest and highest levels (e.g., Wurman et al. 2007b).

2. Deployment overview and data

During the 2012 season of the Radar Observations of Tornadoes and Thunderstorms Experiment (ROTATE; e.g., Wurman 1998, 2008) field campaign, three DOWs, including the RSDOW, and in situ measurement teams deployed in advance of potentially tornadic storms moving toward Russell, Kansas, after dark on 25/26 May 2012. At 0230 UTC 26 May, DOW7[1] was deployed at 38.84195°N, 98.8524°W and the RSDOW deployed at 38.85638°N, 98.8545°W, establishing a 1.6-km, dual-Doppler baseline (Fig. 1). An instrumented mobile mesonet vehicle (P1) carrying "tornado pods" (not deployed) moved north from DOW7.

A tornado formed unexpectedly at 0235 UTC moving northeast, broadening, and impacting P1 at approximately 0238 UTC. The tornado contracted/reformed to the north and then moved northeast, where P1 drove into its southwestern sector just after 0241 UTC. The tornado continued north, with the center passing 30 m east of the RSDOW, resulting in generator failure and ending RSDOW operations.

The tornado transported a house with its resident,[2] located 30 m northeast of the RSDOW, about 30 m eastward, destroying it completely[3] [10 degrees of damage (DOD10) on the enhanced Fujita (EF) scale; Edwards et al. (2013); see Fig. 1]. A nearby house and several other structures were also damaged. At 0242:11 UTC, $V_g = 43$ m s^{-1} was observed by P1[4] at 3.5 m AGL, which experienced the weaker, western side of the tornado core flow. Maximum RSDOW-measured winds, V_d, were 64 m s^{-1} at 6 m AGL[5] at 0240:53 UTC, and the peak velocity difference across the vortex was 113 m s^{-1} at 6 m AGL at 0241:08 UTC. DOW7 observations depicted a low-reflectivity eye and an intermittent debris ring (Fig. 1). The RMW was typically about 50–70 m during the analysis period. The tornado dissipated at ~0243 UTC.

[1] DOWs have 3-dB beamwidths of ~0.9°, oversampled at 0.3°–0.4°, gating at 25 m (RSDOW) and 30 m (DOW7).

[2] P1 crew discovered the resident ~100 s after the event, sitting on the rubble of the transported/destroyed house, suffering from lacerations and a broken collarbone; the crew assisted in her extraction.

[3] The National Weather Service (NWS) rated the tornado EF2.

[4] P1 hosts an R. M. Young 5103 propeller-type anemometer.

[5] Reported DOW observations height adjusted +3 m, accounting for antenna height AGL.

Unauthenticated | Downloaded 02/13/24 12:47 AM UTC

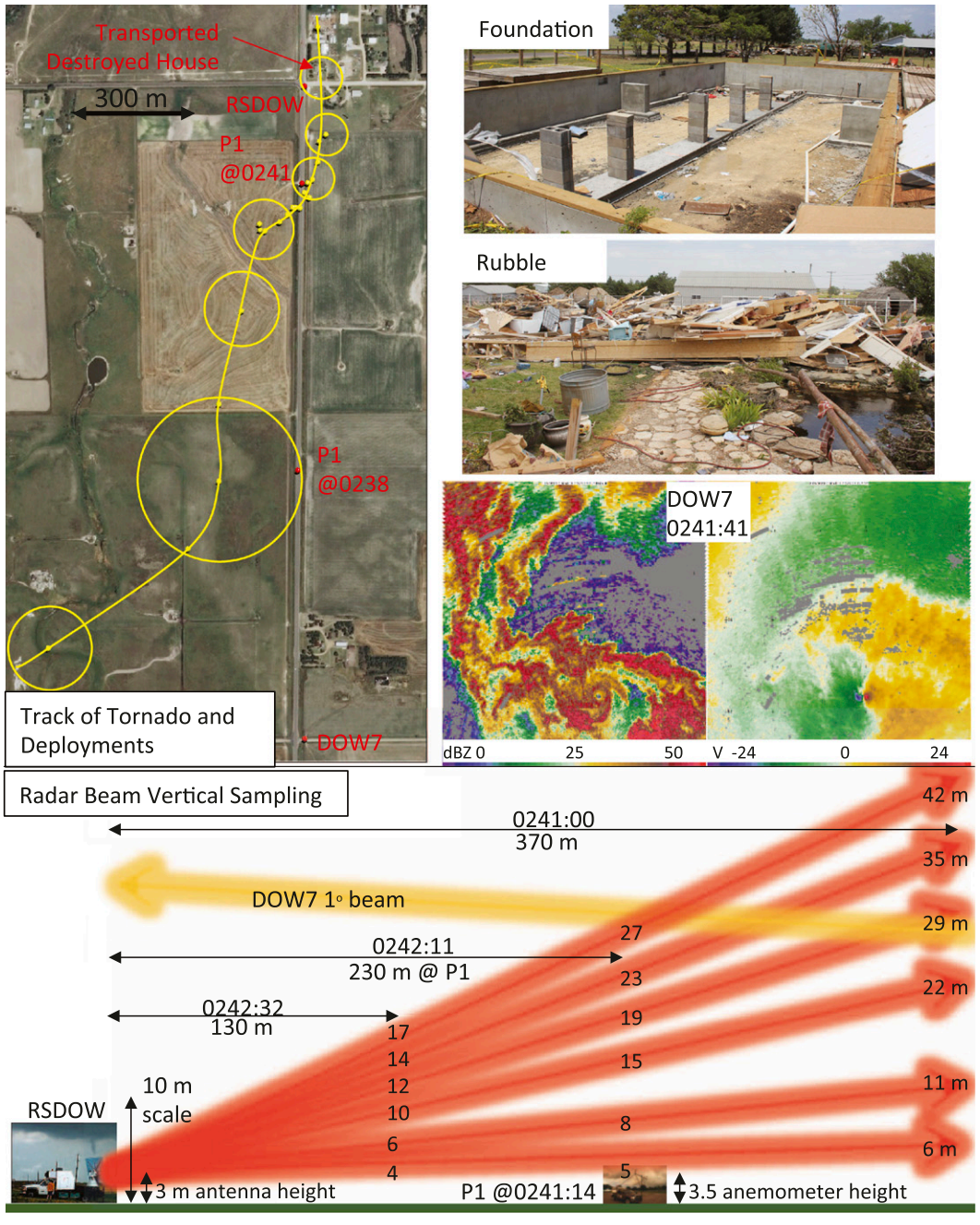

FIG. 1. Moving clockwise from top left: path of the tornado and schematic core flow areas (yellow line and circles) and radar-indicated centers (yellow dots) with DOW7, RSDOW, and P1 locations shown by red dots; photos of the foundation and rubble of a destroyed house; DOW7 reflectivity and velocity in hook echo and tornado; and a schematic of vertical sampling by RSDOW and DOW7 (beam heights, m) with the location of P1's 43.2 m s^{-1} in situ observation indicated.

The proximity of the RSDOW to the tornado (~130 m to the circulation center at the last data collection time, 0242:32 UTC) and six simultaneous radar beams resulted in mapping of the TBL with unprecedented spatial (25-m range and 3-m beamwidth with 1-m oversampling) and temporal resolution (7-s volumes) and proximity to the ground (simultaneous slices as low as 4, 6, 10, 12, 14, and 17 m AGL), well resolving the three-dimensional structure and evolution of the TBL for the first time (Figs. 2 and 3).

GBVTD analyses using 7-s RSDOW volumes from 0240:53 to 0242:25 UTC yielded independent

Unauthenticated | Downloaded 02/13/24 12:47 AM UTC

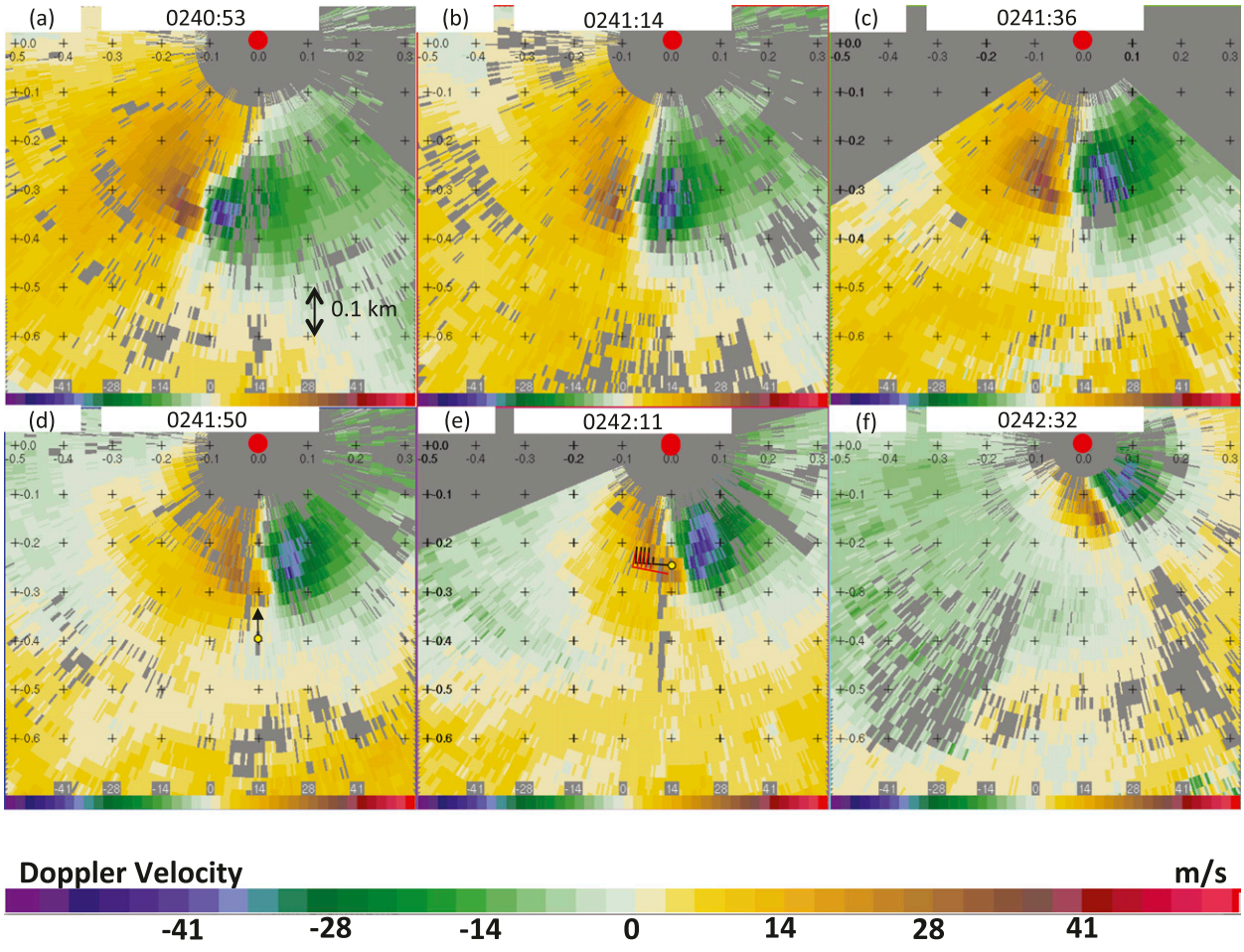

FIG. 2. RSDOW Doppler velocity at six different GBVTD analysis times. (a)–(e) The second lowest elevation angle (7–11 m AGL at tornado) and (f) is at the highest elevation angle (17 m AGL at tornado). Times in hours (HH), minutes (MM), and seconds (ss) (HHMM: ss UTC) indicate the radar beam crossing through the tornado. Red dots indicate the location of the RSDOW. Tick marks indicate every 0.1 km. Yellow circles in (d),(e) show P1 (detected as moving clutter gates, confirmed by GPS, and deleted). Wind barbs in (e) depict the P1 in situ observations at 0241:14 UTC (long barb is 10 m s^{-1} and the short barb is 5 m s^{-1}). Raw wind observation is shown in black. P1 location and wind vector adjusted for tornado translation between the radar and the anemometer observation (red).

three-dimensional wind fields at 14 times (Fig. 5).[6] The sensitivity of the results to objective analysis parameters, lower boundary conditions, and errors in the center location[7] was explored. The vortex structure was not altered substantially by changes in the grid spacing[8] from 2 to 10 m, with only a slight reduction in V_t at grid spacing = 10 m. Small changes in tornado center determination also did not impact the results substantially; an alternate, no-slip, lower-boundary condition reduced V_t below the lowest observation level, but did not alter the vortex structure. The sensitivity to a simple inclusion of debris centrifuging is discussed below.

3. Results and discussion

The maximum V_d from each RSDOW scan[9] and objectively analyzed grid was normalized to V_d (10 m AGL). Peak V_d was observed at the lowest radar-observed level,

[6] RSDOW data were objectively analyzed onto a Cartesian grid using a Barnes scheme (Barnes 1964), grid spacing (radius of influence) of 5 (10) m and 2 (3) m in the horizontal and vertical directions, respectively. Tornado translational motion was subtracted from V_d. Tornado centers were vertically aligned, eliminating tilting errors, but not correcting for flow asymmetries. Vertical winds (w) were derived by the upward integration of the continuity equation, assuming $w(z = 0) = 0$ m s^{-1} and free slip.

[7] Errors in vortex center location were <7 m.

[8] Grid spacing (δ) = Δ/2.5 (where Δ is the raw data spacing) (Koch et al. 1983).

[9] It is likely that $V_g > V_d$ because V_d only captures the component of motion toward–away from the radar.

Unauthenticated | Downloaded 02/13/24 12:47 AM UTC

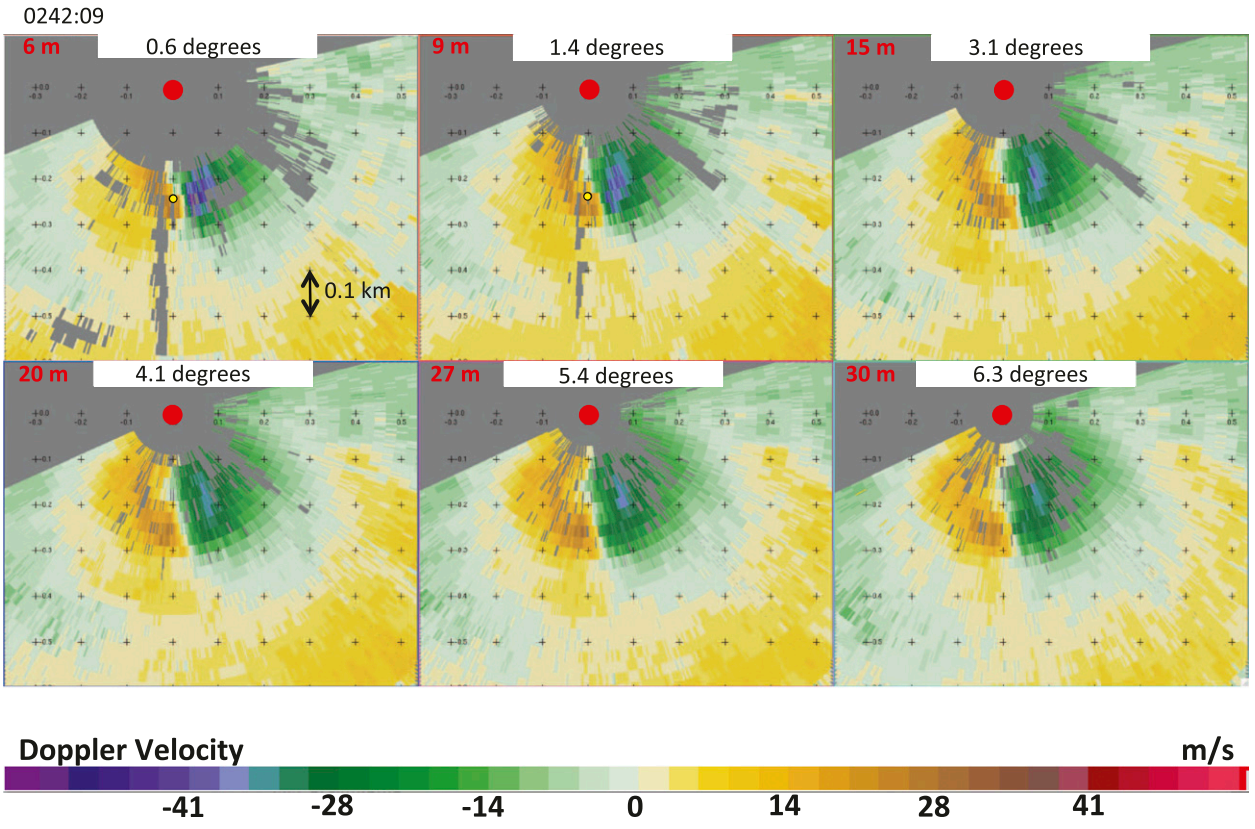

FIG. 3. RSDOW Doppler velocity at six simultaneously observed levels through the tornado at 0242:11 UTC. Fields and annotations are as in Fig. 2. The most intense Doppler velocities are observed at the lowest elevations. The range to the first useful gate is less in higher-elevation beams. Heights of tornado center are indicated in red.

4–6 m AGL, at all times except 0241:14 and 0241:21 UTC, when the maximum was observed at 10 m AGL (Fig. 4). At most times (and in the median and mean profiles), peak V_d decreased ~15% from 5 to 10 m AGL, then gradually decreased another ~10% up to 25–40 m AGL, matching the trend noted from 14 to 100 m AGL in W07, and consistent with V_g (3.5 m AGL) > V_d (30 m AGL) reported in W13. This indicates that the "nose" (maximum) of V_g was very near 5 m AGL and that the true shallow TBL radial inflow was mapped here in detail for the first time. The strongest inflow may even exist below 5 m AGL, where further frictional reduction of V_t could lead to an imbalance in the pressure-gradient force, causing enhanced inflow. Temporal variations in V_d likely were due to true changes in vortex intensity as the tornado is observed by both the DOW7 and RSDOW to rapidly strengthen then rapidly dissipate. In situ anemometer observations from P1, with peak $V_g = 43.2\,\mathrm{m\,s^{-1}}$ at the edge of the western (weak) edge of the core flow region,[10] were roughly consistent with or slightly higher than observational-angle-adjusted V_d at 5 m AGL over P1 (Fig. 2e),[11] corroborating that the maximum V_g occurred near or possibly below 5 m AGL. Critically, this result shows that radar observations of V_d at ~50 m AGL (e.g., WG00, AW05, W07, W13) are likely underestimations of the V_g typically occurring at 5–10 m AGL. However, comparing radar-measured V_d to hypothetical "standard" 3-s-averaged anemometer-measured V_g is problematic.[12]

At all analysis times, GBVTD results revealed a two-celled tornado vortex structure, with a downdraft inside the RMW extending from the top of the domain to the surface. Near-surface inflow, just outside of the

[10] P1 drove into the western side of the tornado after the tornado center had moved east of the road.

[11] P1 is visible as moving ground clutter in the lowest RSDOW sweeps.

[12] Radar measurements are instantaneous and represent reflectivity-weighted averages of scatterer (rain/debris, with associated terminal/centrifuging velocities) motion, usually determined using pulse-pair or spectrally based signal processing techniques, over spatial volumes not equal to 3-s air parcel trajectories.

Unauthenticated | Downloaded 02/13/24 12:47 AM UTC

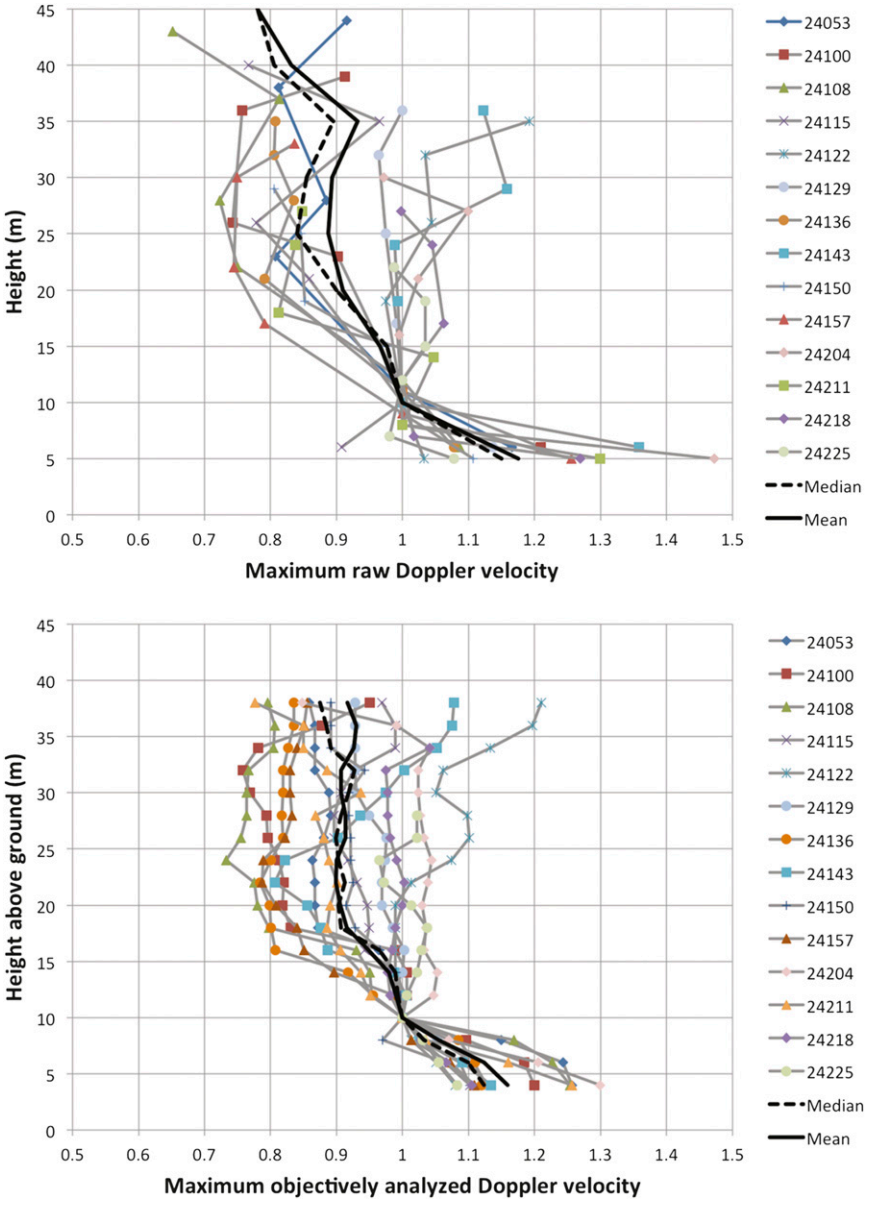

FIG. 4. (top) Maximum RSDOW Doppler velocity in the tornado as a function of height normalized by the 10 m AGL value and (bottom) maximum objectively analyzed RSDOW Doppler velocity as a function of height normalized by the 10 m AGL value for all 14 RSDOW volumes (time labels HMMss UTC, where H indicates hours). Stippled and solid lines depict the median and the mean for all times, respectively. Most intense winds are observed near 5 m AGL, decreasing about 15% by 10 m AGL, then decreasing about another 10% from 10 to 40 m AGL.

RMW, was present in all but the last three analysis times (Figs. 5 and 6). Maximum inflow occurred at 0240:53 UTC, near the time of maximum V_d and V_t. At 0240:53 UTC, $V_r < -1\,\mathrm{m\,s^{-1}}$ was present ≤ 14 m AGL, while $V_r < -5\,\mathrm{m\,s^{-1}}$ was confined to ≤ 8 m AGL, with the strongest inflow (V_r of approximately $-7\,\mathrm{m\,s^{-1}}$) at 5 m AGL. P1 observations at 0241:14 UTC, adjusted for tornado translation and motion, result in a tornado-relative velocity of $42.9\,\mathrm{m\,s^{-1}}$ from 281° (Fig. 2), suggesting slight inflow, $V_r < 0$, while the GBVTD at this time suggests slight outflow, $V_r > 0$ (Figs. 5 and 6). This discrepancy could be caused by inadequate compensation for debris centrifuging, errors in correcting for tornado movement, asymmetries in the tornado, stronger inflow <5 m AGL, errors in the wind or radar measurements, or a combination of these factors.

Unauthenticated | Downloaded 02/13/24 12:47 AM UTC

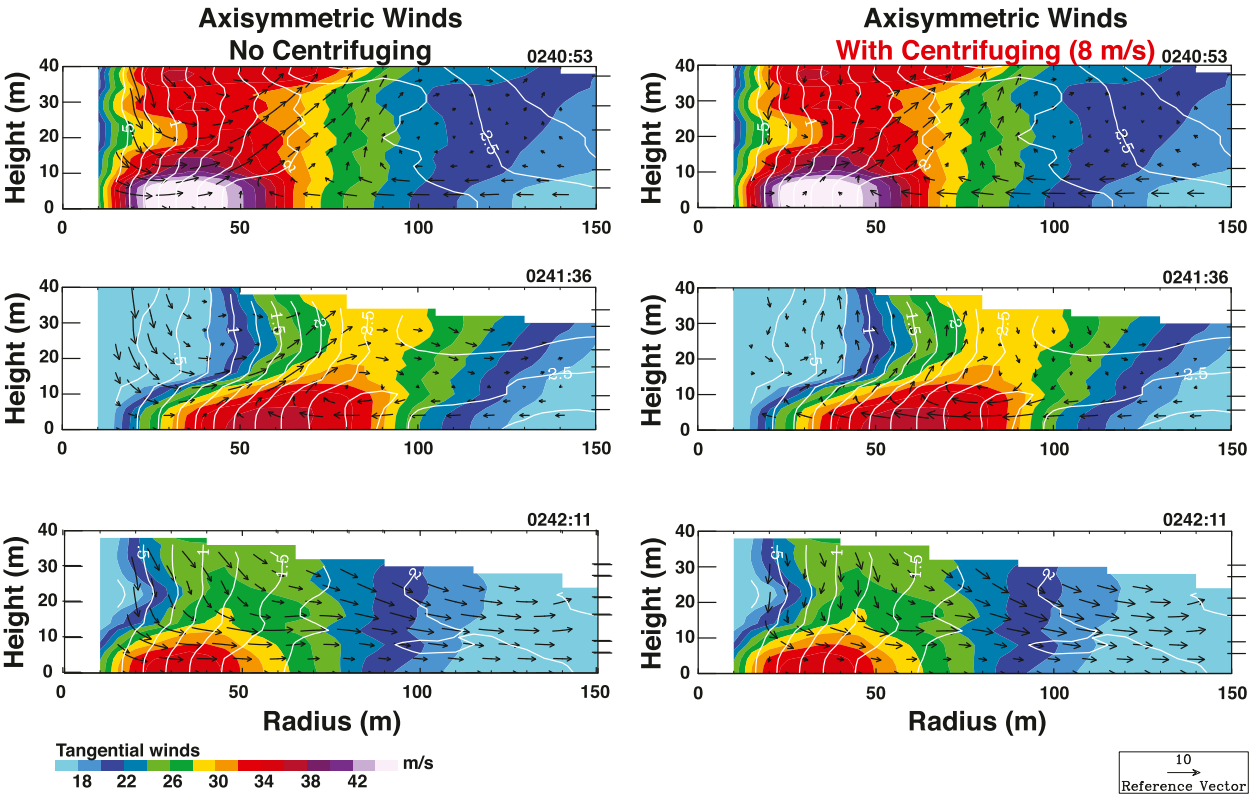

FIG. 5. GBVTD winds at (top) 0240:53, (middle) 0241:36, and (bottom) 0242:11 UTC with (left) no centrifuging and (right) an 8 m s^{-1} centrifuging estimation. Colored contours depict the tangential velocity V_t, vectors depict the secondary circulation (V_r, w), and white line contours depict the angular momentum ($\times 10^3$ m^2 s^{-1}). Tick marks along the right axes denote the heights of RSDOW sweeps through the center of the tornado. The 0242:11 UTC analysis is just prior to the P1 in situ observation of 43.2 m s^{-1}.

The value of V_t was maximum in the TBL, below ~6 m AGL (Fig. 6). By 0241:00 UTC, the depth of the inflow layer ($V_r < -1$ m s^{-1}) had decreased to 10 m AGL and the layer containing $V_r < -4$ to -5 m s^{-1} decreased to <6 m AGL. From 0241:00 to 0241:22 UTC, the depth of the inflow layer was ~10 m AGL, and V_r and V_t generally decreased in magnitude. At 0241:29 UTC, there was a brief increase in the $V_r < 0$ and V_t, subsequently followed by a decrease in V_t until 0242:11 UTC, when V_t increased until the end of the analysis. Although V_t increased from 0242:11 to 0242:25 UTC, outflow $V_r > 0$ was present outside the RMW and the tornado dissipated approximately 60 s later. Strong V_t immediately prior to tornado dissipation has been documented before (e.g., WG00, Kosiba et al. 2013).

Since there is not adequate information on precisely how debris can bias Doppler velocity measurements, an exact quantification of debris centrifuging is beyond the scope of this study. However, using the results of Dowell et al. (2005) and W12, Nolan (2013) provides a simple estimate of debris-centrifuging biases on retrieved axisymmetric winds. Following Nolan (2013) [Eq. (3.1)], and consistent with the values presented in W12 and Dowell et al. (2005), $V_c = 8$ m s^{-1} was used in this study since this was a weak tornado and likely only hydrometeors and small debris, such as dirt, gravel, and grass[13] were present throughout the GBVTD analysis interval as the tornado crossed open farm and grassland[14] prior to impacting the structures near the RSDOW. Including an estimate for debris centrifuging moved the location of maximum convergence inward (Fig. 6) and caused the weak central downdraft near the surface to become a weak central updraft at 0241:22–0241:43 and 0241:57–0242:04 UTC. Indeed, with the inclusion of a simple debris bias, the inward progression of the radial winds is consistent with the LES results of LL00. The sign of V_r outside of the RMW was not changed by the inclusion of

[13] Since the observations were close to the surface, dirt, gravel, and/or grass likely were appreciable scatter types in the radar sample volumes. The in situ P1 crew did not report airborne debris hitting their vehicle.

[14] The surface roughness length was approximated as 0.1 m, characteristic of "openly rough" terrain (Davenport et al. 2000).

Unauthenticated | Downloaded 02/13/24 12:47 AM UTC

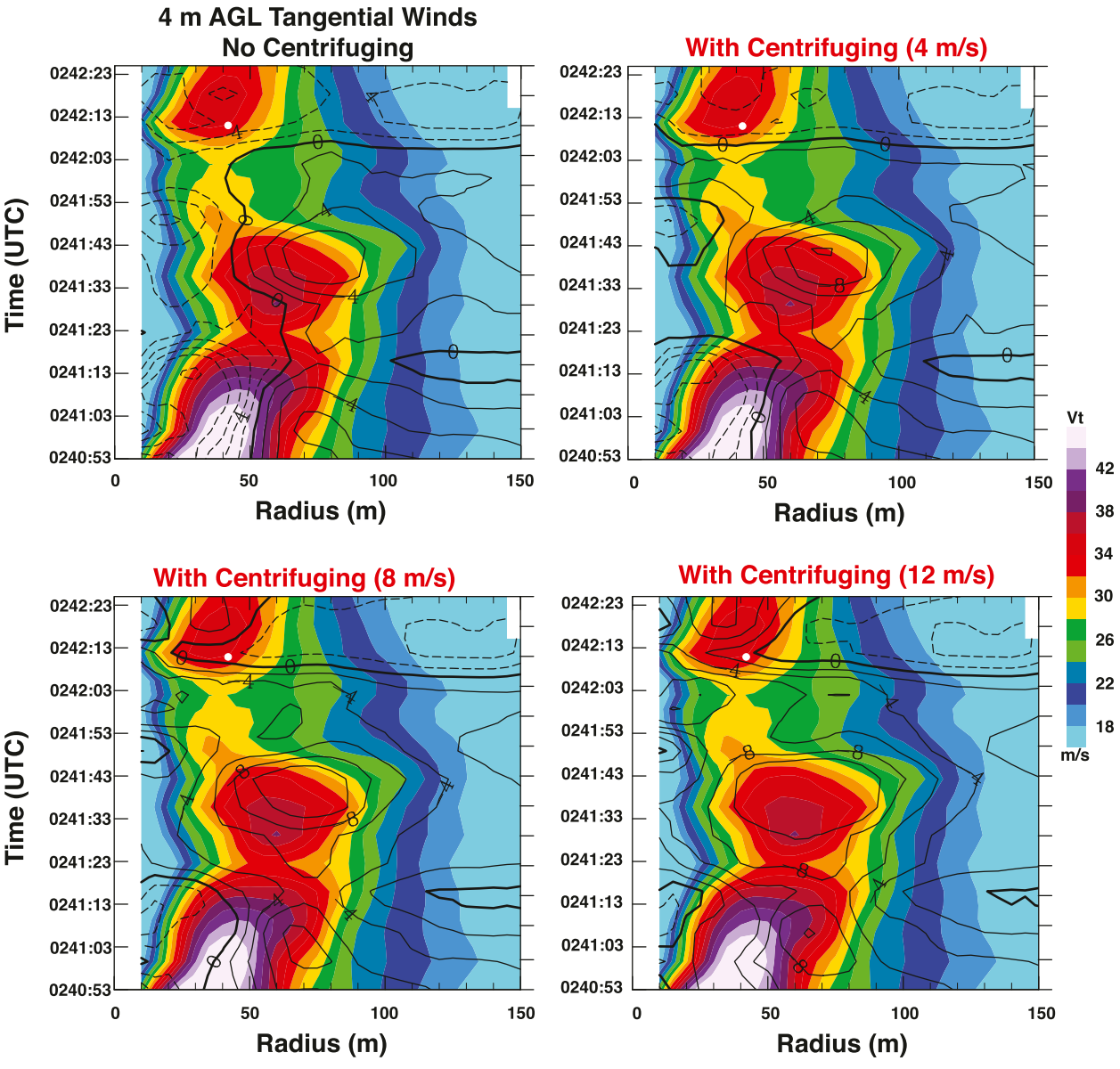

FIG. 6. Hovmöller diagrams of the axisymmetric horizontal winds in the TBL as a function of radius and time (top left) with no centrifuging, and 4, 8, and 12 m s^{-1} V_{cf} at 4 m AGL. Colored contours depict the tangential velocity V_t and radial inflow (outflow) V_r is denoted by solid (stippled) lines. Tick marks along the right axes denote times of RSDOW volumes. A downdraft/outflow is present inside the RMW at all times with no centrifuging and only at the early times when centrifuging is included. Inflow outside of the RMW is present through 0242:11 UTC, with outflow afterward, in all analyses. The location and time of the P1 in situ observation ($V_r = -4.3$ m s^{-1} and $V_t = 42.9$ m s^{-1}) are shown with a white dot.

debris (Fig. 5). Since one unknown in accounting for debris centrifuging is the size, shape, and density distribution of the debris–hydrometeor mix, and hence V_{cf}, sensitivity of the results to varying V_{cf} (4 and 12 m s^{-1}) was explored (Figs. 6c and 6d). As expected, the higher (lower) value increased (decreased) inflow and allowed the inflow to penetrate farther (less far) inward. The central updraft–downdraft responded according to changes in the inflow.

The depth of the inflow layer was much shallower than has been reported in previous studies (e.g., LW05, K08, KW10, W12), but these results were based completely or primarily on data well *above* the shallow TBL revealed here. W12, KW10, K08, and LW05 employed vertical grid spacings of 50, 40, 25, and 30 m, respectively, so these likely did not resolve very-near-surface inflow, but instead captured the large-scale inflow associated with the wind field outside the core flow region of the tornado, or

Unauthenticated | Downloaded 02/13/24 12:47 AM UTC

a smoothed representation of inflow below their lowest analysis level. The weaker inflow revealed here compared to the analyses of LW05, K08, KW10, and W13 may be due to the resolution of the true TBL or because the current tornado was weaker and short lived, with low-level inflow not conducive to sustaining an intense, long-lived vortex (L00).

In the LESs of L00 and LL07, a corner flow swirl ratio[15] S_c has been defined to characterize the impacts of near-surface, tornado-scale flow on vortex structure and intensity. While S_c does not replace the outer-scale swirl ratio S_o (e.g., Church et al.1979; Lee and Wurman 2005), S_c underscores the importance of near-surface flow structure, which is not captured by S_o.[16] At the "optimal" S_c value (S_c = 0.70–1.38; LL07), the ratio of the average maximum swirl velocities (V_{max}) in the surface layer to the average swirl velocities above the surface layer (V_c) is 2.5 (L00). In the current analysis, values of V_{max} (z = 4 m AGL)/V_c (z = 20 m AGL) < 1.5. The highest values (V_{max}/V_c = 1.37–1.47) occurred at the first three analysis times. The lowest values (~1.0) were observed at 0241:22, 0242:04, 0242:18, and 0242:25 UTC, when the angular momentum outside of the RMW was reduced in the TBL, perhaps indicating an influx of far-field lower angular momentum fluid near the surface, decreasing the tornado intensity. Using quantities available in the GBVTD domain, and only for times when $V_r < 0$ was observed, $S_c \gg 1$,[17] so S_c would have to either decrease (assuming an unchanged flow aloft) or stayed fixed (if the core radius aloft was reduced) in order for the vortex to intensify.[18]

4. Conclusions

The TBL and inflow layer were much shallower than previously documented, confined below 10–14 m AGL. While it is possible that more intense tornadoes may have deeper boundary and inflow layers, it is likely that prior observational studies characterized the inflow layer of the larger-scale circulation, not of the tornado itself. Estimation of S_c predictions from the current data are consistent with LES results. A two-celled vortex structure is revealed by GBVTD analysis without the inclusion of debris centrifuging, and outflow outside the RMW was observed just prior to tornado dissipation. Inclusion of varied estimates for debris centrifuging changed weak downdrafts to very weak updrafts inside the RMW and the flow direction outside of the RMW was unaltered.

The most intense winds in the tornado occurred ~5 m AGL, extending surfaceward the results of previous studies sampling above the TBL (e.g., W05, W07) or sparsely within the TBL (W13). Radar-observed V_d a few 10 s of meters AGL are shown to be representative or even underestimates of V_g approximately <10 m AGL. More observations are needed over a range of vortex structures and intensities to characterize the TBL more generally.

Acknowledgments. Analysis supported by NSF-AGS-0910737 and DOWs by NSF-AGS-0801041. We thank Curtis Alexander, Paul Robinson, and Rachel Humphrey.

[15] Here, $S_c = r_c\Gamma_\infty/\Upsilon$, where r_c is a characteristic radius of V_t(max), Γ_∞ is the ambient angular momentum, and Υ is the depleted angular momentum flux in the surface layer.

[16] Note that S_o characterizes the flow in which the tornado forms. Both S_o and S_c are difficult to define in nature since flow parameters are not easily defined. In addition, S_o cannot be approximated in the current study since the analysis domain is too small to define the large-scale flow in which the tornado is embedded.

[17] Assuming r_c = 60 m, $\Gamma_\infty = 3.0 \times 10^3\ m^2\ s^{-1}$, and $\Upsilon = 1.0 \times 10^3\ m^5\ s^{-2}$.

[18] Values of parameters composing S_c are uncertain, but reasonable choices yield $S_c \gg 1$.

REFERENCES

Alexander, C., and J. Wurman, 2005: The 30 May 1998 Spencer, South Dakota, storm. Part I: The structural evolution and environment of the supercell tornadoes. *Mon. Wea. Rev.,* **133,** 72–96.

Barnes, S. L., 1964: A technique for maximizing details in numerical weather-map analysis. *J. Appl. Meteor.,* **3,** 396–409.

Bluestein, H. B., W.-C. Lee, M. Bell, C. C. Weiss, and A. L. Pazmany, 2003: Mobile Doppler radar observations of a tornado in a supercell near Bassett, Nebraska, on 5 June 1999. Part II: Tornado-vortex structure. *Mon. Wea. Rev.,* **131,** 2968–2984.

——, C. C. Weiss, and A. L. Pazmany, 2004: The vertical structure of a tornado: High-resolution, W-band, Doppler radar observations near Happy, Texas, on 5 May 2002. *Mon. Wea. Rev.,* **132,** 2325–2337.

Church, C. R., J. T. Snow, G. L. Baker, and E. M. Agee, 1979: Characteristics of tornado-like vortices as a function of swirl ratio: A laboratory investigation. *J. Atmos. Sci.,* **36,** 1755–1776.

Davenport, A. G., C. S. B. Grimond, T. R. Oke, and J. Wieringa, 2000: Estimating the roughness of cities and sheltered country. Preprints, *12th Conf. on Applied Climatology,* Asheville, NC, Amer. Meteor. Soc., 96–99.

Davies-Jones, R. P., R. J. Trapp, and H. B. Bluestein, 2001: Tornadoes and tornadic storms. *Severe Convective Storms, Meteor. Monogr.,* No. 50, Amer. Meteor. Soc., 167–221.

Dowell, D. C., C. R. Alexander, J. M. Wurman, and L. J. Wicker, 2005: Centrifuging of hydrometeors and debris in tornadoes: Radar-reflectivity patterns and wind-measurement errors. *Mon. Wea. Rev.,* **123,** 1501–1524.

Edwards, R., J. G. LaDue, J. T. Ferree, K. Scharfenberg, C. Maier, and W. L. Coulbourne, 2013: Tornado intensity estimation: Past, present, and future. *Bull. Amer. Meteor. Soc.,* **94,** 641–653.

Hoecker, W. H., 1960: Wind speed and air flow patterns in the Dallas tornado of April 2, 1957. *Mon. Wea. Rev.,* **88,** 167–180.

Kessler, E., 1986: *Thunderstorm Morphology and Dynamics.* Vol. 2, *Thunderstorms: A Social, Scientific, and Technological Documentary,* University of Oklahoma Press, 432 pp.

Unauthenticated | Downloaded 02/13/24 12:47 AM UTC

Koch, S. E., M. desJardins, and P. J. Kocin, 1983: An interactive Barnes objective map analysis scheme for use with satellite and conventional data. *J. Climate Appl. Meteor.,* **22,** 1487–1503.

Kosiba, K. A., and J. Wurman, 2010: The three-dimensional axisymmetric wind field structure of the Spencer, South Dakota, 1998, tornado. *J. Atmos. Sci.,* **67,** 3074–3083.

——, R. J. Trapp, and J. Wurman, 2008: An analysis of the axisymmetric three-dimensional low-level wind field in a tornado using mobile radar observations. *Geophys. Res. Lett.,* **35,** L05805, doi:10.1029/2007GL031851.

——, J. Wurman, P. Markowski, Y. Richardson, P. Robinson, and J. Marquis, 2013: Genesis of the Goshen County, Wyoming, tornado on 5 June 2009 during VORTEX2. *Mon. Wea. Rev.,* **141,** 1157–1181.

Lee, W.-C., and J. Wurman, 2005: Diagnosed three-dimensional axisymmetric structure of the Mulhall tornado on 3 May 1999. *J. Atmos. Sci.,* **62,** 2373–2393.

——, B. J.-D. Jou, P.-L. Chang, and S.-M. Deng, 1999: Tropical cyclone kinematic structure retrieved from single-Doppler radar observations. Part I: Doppler velocity patterns and the GBVTD technique. *Mon. Wea. Rev.,* **127,** 2419–2439.

Lewellen, D. C., and W. S. Lewellen, 2007: Near-surface intensification of tornado vortices. *J. Atmos. Sci.,* **64,** 2176–2194.

——, ——, and J. Xia, 2000: The influence of a local swirl ratio on tornado intensification near the surface. *J. Atmos. Sci.,* **57,** 527–544.

——, B. Gong, and W. S. Lewellen, 2008: Effects of finescale debris on near-surface tornado dynamics. *J. Atmos. Sci.,* **65,** 3247–3262.

Lewellen, W. S., 1976: Assessment of knowledge and implications for man. *Proc. Symp. on Tornadoes,* Lubbock, TX, Texas Tech University, 107–143.

——, 1993: Tornado vortex theory. *The Tornado: Its Structure, Dynamics, Prediction and Hazards, Geophys. Monogr.,* Vol. 79, Amer. Geophys. Union, 19–39.

——, D. C. Lewellen, and R. I. Sykes, 1997: Large-eddy simulation of a tornado's interaction with the surface. *J. Atmos. Sci.,* **54,** 581–605.

Nolan, D. S., 2013: On the use of Doppler radar–derived wind fields to diagnose the secondary circulations of tornadoes. *J. Atmos. Sci.,* **70,** 1160–1171.

Snow, J. T., 1982: A review of recent advances in tornado vortex dynamics. *Rev. Geophys. Space Phys.,* **20,** 953–964.

Tanamachi, R. L., H. B. Bluestein, W.-C. Lee, M. Bell, and A. Pazmany, 2007: Ground-based velocity display (GBVTD) analysis of W-band Doppler radar data in a tornado near Stockton, Kansas, on 15 May 1999. *Mon. Wea. Rev.,* **135,** 783–800.

Wakimoto, R. M., P. Stauffer, W.-C. Lee, N. T. Atkins, and J. Wurman, 2012: Finescale structure of the LaGrange, Wyoming, tornado during VORTEX2: GBVTD and photogrammetric analyses. *Mon. Wea. Rev.,* **140,** 2939–2958.

Wurman, J., 1998: Preliminary results and report of the ROTATE-98 tornado experiment. Preprints, *19th Conf. on Severe Local Storms,* Minneapolis, MN, Amer. Meteor. Soc., 120–123.

——, 2001: The DOW mobile multiple Doppler network. Preprints, *30th Int. Conf. on Radar Meteorology,* Munich, Germany, Amer. Meteor. Soc., 95–97.

——, 2008: Preliminary results and report of the ROTATE-2008 radar/in-situ/mobile mesonet experiment. *Proc. 24th Conf. on Severe Local Storms,* Savannah, GA, Amer. Meteor. Soc., 5.4. [Available online at https://ams.confex.com/ams/24SLS/webprogram/Paper142200.html.]

——, and S. Gill, 2000: Finescale radar observations of the Dimmitt, Texas, tornado. *Mon. Wea. Rev.,* **128,** 2135–2164.

——, and M. Randall, 2001: An inexpensive, mobile, rapid-scan radar. Preprints, *30th Conf. on Radar Meteorology,* Munich, Germany, Amer. Meteor. Soc., P3.4. [Available online at https://ams.confex.com/ams/pdfpapers/21577.pdf.]

——, and K. Kosiba, 2013: Finescale radar observations of tornado and mesocyclone structures. *Wea. Forecasting,* **28,** 1157–1174.

——, J. Straka, and E. Rasmussen, 1996: Fine-scale Doppler radar observation of tornadoes. *Science,* **272,** 1774–1777.

——, ——, ——, M. Randall, and A. Zahrai, 1997: Design and deployment of a portable, pencil-beam, pulsed, 3-cm Doppler radar. *J. Atmos. Oceanic Technol.,* **14,** 1502–1512.

——, C. Alexander, P. Robinson, and Y. Richardson, 2007a: Low-level winds in tornadoes and potential catastrophic tornado impacts in urban areas. *Bull. Amer. Meteor. Soc.,* **88,** 31–46.

——, Y. Richardson, C. Alexander, S. Weygandt, and P. F. Zhang, 2007b: Dual-Doppler analysis of winds and vorticity budget terms near a tornado. *Mon. Wea. Rev.,* **135,** 2392–2405.

——, D. Dowell, Y. Richardson, P. Markowski, E. Rasmussen, D. Burgess, L. Wicker, and H. B. Bluestein, 2012: The Second Verification of the Origins of Rotation in Tornadoes Experiment: VORTEX2. *Bull. Amer. Meteor. Soc.,* **93,** 1147–1170.

——, K. Kosiba, and P. Robinson, 2013a: In situ, Doppler radar, and video observations of the interior structure of a tornado and the wind–damage relationship. *Bull. Amer. Meteor. Soc.,* **94,** 835–846.

Unauthenticated | Downloaded 02/13/24 12:47 AM UTC